Dynamic light scattering measurements of polystyrene in semidilute theta solutions

Eric J. Amis*, Charles C. Han and Yushiu Matsushita†
National Bureau of Standards, Washington, DC, USA
(Received 1 June 1983)

Measurements of the co-operative diffusion coefficient, D_c, and a centre of mass translational diffusion coefficient, D_s, have been made by dynamic light scattering for the polystyrene–cyclohexane theta system as a function of molecular weight and concentration. For semidilute solutions it is established that $D_s \propto N^{-2} c^{-3}$ which is in agreement with the predictions from scaling arguments for the self-diffusion coefficient. However, if the co-operative mode is interpreted by $D_c \propto N^x c^y$, the results of $0 < x < 0.7$ and $0 < y < 0.5$ are in disagreement with scaling predictions of $D_c \propto N^0 c^1$. A discussion of the assumptions and potential shortcomings of the blob model which is used in the derivation of the power law predictions and the dynamic scattering equations is included. In addition, monomeric friction coefficients have been obtained from the D_s results within the framework of Doi–Edwards model. A comparison is made of the concentration dependence of the monomeric friction coefficient from the present data to that from similar experiments on a good solvent (tetrahydrofuran) system and from shear relaxation modulus measurements on the polystyrene in Aroclor 1248.

(Keywords: dynamic light scattering; semidilute theta solutions; cooperative diffusion; self diffusion; centre of mass transitional diffusion; scaling laws; reptation; monomeric friction coefficient)

INTRODUCTION

Dynamic light scattering (DLS) has proved to be a very useful tool for the study of dilute solutions of polymer molecules. Similarly, in semidilute solutions, dynamic light scattering is important in the testing and refinement of predictions from scaling theory and renormalization group calculations[1]. Most of this work has concentrated on the short time co-operative diffusion coefficient, D_c, of semidilute solutions and gels. Adam and Delsanti[2] were the first to use this technique to measure D_c and to compare the concentration dependence with predictions based on scaling concepts. A number of experiments, all in nominally good solvent conditions, have since been reported with both confirmatory and contradictory results[3–6]. Recently, it has been demonstrated[7] that for semidilute solutions of gelatin above the gelling temperature, the centre of mass motion (as described by the self-diffusion coefficient, D_s) as well as D_c can be measured by DLS. Briefly, those results were obtained by analysing the intensity autocorrelation function of the scattered light with experimental sampling times ranging over several orders of magnitude. The angular dependence of the resulting exponential decay constants produced two distinct and widely separated diffusion coefficients. The fast diffusion coefficient was identified as D_c from its magnitude, concentration dependence and the fact that it remained unchanged upon gelation of the sample. The slow process was identified with the centre of mass motion because it decreased markedly with an increase in concentration (as is predicted for semidilute solutions where reptation presumably controls the single-chain translation[8]) and because this slow process was completely stopped upon crosslinking of the gelatin.

The possibility of measuring D_s in semidilute solutions is very interesting because of the strong dependence on both concentration and molecular weight. With this in mind, similar experiments were recently reported[9] for solutions of well characterized polystyrene in tetrahydrofuran, THF (a good solvent) over extensive concentration ranges for molecular weights from 3.74×10^4 to 5.05×10^6. While these experiments were consistent with the general features of scaling theory and the reptation model as formulated by de Gennes[10] they also emphasized that, for a good solvent, the strict cutoffs and power laws of scaling theory are unrealistic, as had been observed previously[11].

It is possible that in theta solutions there will be better agreement between dynamic scaling law predictions and experimental results, as there is no concentration crossover between good solvent behaviour and theta behaviour. This paper presents measurements of D_c and D_s for polystyrene in theta solvent as a function of concentration and molecular weight. First though, the physical basis for the observation of D_s by DLS is discussed.

THEORY

For dilute solutions the theory of dynamic light scattering has been developed by several different approaches. From each of these theories it is clear that for values of the scattering wavevector $q\left(q = \frac{4\pi}{\lambda} \sin \theta/2\right)$ such that $qR_g < 1$, the short time intensity autocorrelation function yields a mutual diffusion coefficient. For semidilute

* Present address: Department of Chemistry, University of Wisconsin, Madison, WI 53706, USA.
† Present address: Department of Synthetic Chemistry, Nagoya University, Nagoya, Japan.

0032-3861/84/050650-09$03.00

solutions the theory, and agreement, is not so clear. Here, one explanation is presented for the measurement of D_c and D_s by short time and long time measurement of dynamic light scattering. For simplicity, the approach is based on the blob model and the concept of reptation. Although it may not be necessary to be limited to this model, it is chosen because it allows examination of the predictions for effects of concentration, molecular weight and solvent quality on D_c and D_s under one unified framework. As the scattering equations are based in part on the assumptions involved in scaling and reptation it is not possible to prove or disprove their correctness but rather the consistency of the model's predictions with the experimental results, is examined.

Co-operative diffusion, D_c

In the blob model[1,2], the single-chain excluded volume effect is modelled as:

$$\langle R_{ij}^2\rangle = l^2(|i-j|)^{2\nu} \quad \text{for } |i-j|<N_\tau$$

and

$$= \xi_\tau^2\left(\frac{|i-j|}{N_\tau}\right)^{2\nu} = l^2 N_\tau^{1-2\nu}|i-j|^{2\nu} \quad \text{for } |i-j|>N_\tau \tag{1}$$

where

$$\nu = 3/5 \text{ for } |i-j|>N_\tau$$

and

$$\nu = 1/2 \text{ for } |i-j|<N_\tau$$

Here N_τ is the number of monomers, of length l, within the cutoff length of the 'temperature blob' which has a Gaussian-like distribution and end-to-end distance of ξ_τ ($\xi_\tau^2 = l^2 N_\tau$). As the concentration increases, polymers start to overlap and a crossover to the semidilute region is defined at concentration $c^* \equiv M/N_A R_g^3$. In this region a new distance scale ξ_c is introduced with a new 'concentration blob, 'length N_c with:

$$\langle R_{ij}^2\rangle = \xi_c^2\left(\frac{|i-j|}{N_c}\right)^{2\nu} \tag{2}$$

where

$$\nu = 1/2 \text{ for } |i-j|>N_c$$

and $\xi_c^2 \equiv \langle \xi_c^2\rangle$ follows the single-chain mean square distance distribution as in equation (1). Over distances of ξ_c, the section of a polymer chain of length N_c monomers can be considered as an independent strand with other chains screening out both the excluded volume and hydrodynamic interaction from monomers of other sections of the same chain.

Normally, it is possible to visualize the physical situation by starting from a single chain at a temperature $T \gg \theta$. This is a single chain ($N_c \to \infty$) with fully developed excluded volume ($N_\tau = 1$). As concentration increases to and beyond c^*, N_c decreases and becomes smaller than the degree of polymerization N. The chain is thus a 'rescaled Rouse chain' with bead size N_c monomers. Under these conditions, a co-operative diffusion coefficient can be defined as:

$$D_c = \frac{kT}{6\pi\eta_0\xi_c} \tag{3}$$

In the extreme cases of θ condition ($N_\tau \to \infty$) and fully developed excluded volume condition ($N_\tau = 1$), the scaling theory predicts $\xi_c \propto c^{-\nu/3\nu-1}$ and, therefore:

$$D_c \propto N^0 c^{+0.75} \text{ (good solvent)}$$

$$\propto N^0 c^{+1.0} \text{ (θ solvent)} \tag{4}$$

For an intermediate condition of moderate temperature (solvent quality) and semidilute concentration ($N > N_c > N_\tau > 1$) a polymer chain should have Gaussian behaviour at distances, d, larger than ξ_c, excluded volume behaviour at $\xi_c > d > \xi_\tau$ and Gaussian behaviour again at $d < \xi_\tau$. It is, therefore, important to realize that the quantity measured by an experimental technique can be sensitive to the distance scale (q^{-1} in the scattering experiment) probed by the experiment. As it is possible for ξ_c to be equal to or smaller than ξ_τ at finite solvent concentrations, the crossovers between Gaussian and excluded volume behaviour due to both temperature and concentration have made experimental tests of scaling theory very difficult and sometimes confusing.

Self diffusion, D_s

The concept of reptation was postulated by de Gennes to describe the motion of the centre of mass of an individual polymer chain within a semidilute solution. In a semidilute solution, a polymer chain may move more readily in its longitudinal direction, along its contour, than in the lateral direction because of the interference by other chains which surround it. The diffusion coefficient in the longitudinal direction or along the so called 'tube' defined by foreign monomers may be written as:

$$D_t = \frac{kT}{6\pi\eta_0\xi_c}\frac{N_c}{N} \tag{5}$$

The curvilinear length of the tube in terms of the distance ξ_c is given as $L = (N/N_c)\xi_c$. If the time for the chain to completely redefine its configuration by reptation is t_R, then:

$$D_t t_R \propto L^2 \tag{6}$$

and

$$t_R \propto \frac{6\pi\eta_0}{kT}\left(\frac{N}{N_c}\xi_c\right)^3 \tag{7}$$

by noting that $N_c \propto c\xi_c^3$ it follows that

$$t_R \propto N^3 c^{3/2} \text{ (good solvent)}$$

and

$$\propto N^3 c^3 \text{ (θ solvent)} \tag{8}$$

During the time t_R the centre of mass of the chain actually diffuses in a three-dimensional random walk a distance R related by the self-diffusion coefficient D_s as:

$$6D_s t_R = R^2 \tag{9}$$

where R is the chain end-to-end distance. As $R^2 \propto Nc^{-1/4}$ in good solvent and $R^2 \propto Nc^0$ in θ solvent:

$$D_s \propto N^{-2}c^{-1.75} \text{ (good solvent)}$$

$$\propto N^{-2}c^{-3} \text{ (θ solvent)} \tag{10}$$

Dynamic light scattering

The intermediate scattering function $S(q,t)$ in a dynamic scattering experiment, can be written as:

$$S(q,t) = \langle \rho^*(0)\rho(t)\rangle \tag{11}$$

with

$$\rho(t)=\sum_j e^{iqR_j(t)} \tag{12}$$

In the semidilute solution, j sums through all monomers from different polymers and from different strands or blobs of the same polymer. As previously, a strand is taken to be a section of the polymer chain of length N_c monomers. In the case of $t \ll t_R$ and $q\xi_c < 1$:

$$S(q,t)=\left\langle \sum_{p=p'} e^{iq\cdot(R_p(0)-R_{p'}(t))} \sum_{s=s'} e^{iq\cdot(R_{ps}(0)-R_{p's'}(t))} \sum\sum_{m\ m'} e^{iq\cdot(R_{sm}(0)-R_{s'm'}(t))} \right.$$

$$+ \sum_{p=p'} e^{iq\cdot(R_p(0)-R_{p'}(t))} \sum_{s\neq s'} e^{iq\cdot(R_{ps}(0)-R_{p's'}(t))} \sum\sum_{m\ m'} e^{iq\cdot(R_{sm}(0)-R_{s'm'}(t))}$$

$$\left. + \sum_{p\neq p'} e^{iq\cdot(R_p(0)-R_{p'}(t))} \sum\sum_{s\ s'} e^{iq\cdot(R_{ps}(0)-R_{p's'}(t))} \sum\sum_{m\ m'} e^{iq\cdot(R_{sm}(0)-R_{s'm'}(t))} \right\rangle \tag{13}$$

where the subscripts p, s and m enumerate the sums over polymers, strands within a single polymer and monomers within a single strand, respectively. The three terms can be identified as follows. The first term is the correlation of each monomer with others from the same strand. The second is the correlation of every monomer with others from each different strand of the same polymer. The third term is the correlation of every monomer with each monomer from each strand of every different polymer. For example, R_{ps} is the vector from the centre of mass of polymer p to the centre of mass of strand s. When $t \ll t_R$ and $q\xi_c < 1$, $R_p(t) \approx R_p(0)$ and $e^{iq\cdot R_{sm}(0)} \approx e^{iq\cdot R_{s'm'}(t)} \approx 1$. Also, as the temporary network model was assumed in the scaling approach, it follows that the motions of different strands are uncorrelated. The scattering function in equation (13) thereby reduces to:

$$S(q,t)=N_pN_c^2\left\langle \sum_{s=s'} e^{iq\cdot(R_{ps}(0)-R_{ps'}(t))} \right\rangle$$

$$+N_p\langle\rho'_s(0)\rangle^2\langle\rho_m\rangle^2+\langle\rho'_p\rangle^2\langle\rho_s\rangle^2\langle\rho_m\rangle^2$$

$$\approx N_pN_c^2N_se^{-q^2D_c(1-\phi)t}+S_c(q) \tag{14}$$

where $S_c(q)$ is a time independent function, ϕ is the polymer volume fraction, N_p, N_s, and N_c are the number of polymers, number of strands per polymer and number of monomers per strand, respectively, and $\langle\rho'_s\rangle$ and $\langle\rho'_p\rangle$ are the restricted sums over all strands and polymer chains. Note that the density averages, $\langle\rho'_s\rangle$, $\langle\rho_s\rangle$, $\langle\rho'_p\rangle$ and $\langle\rho_m\rangle$ are all time independent functions at this short time scale, thus $S_c(q)$ is used to represent this q dependent but time independent part.

In the case $t \gg t_R$ and $qR_g < 1$, the loss of memory at distances greater than ξ_c cannot be assumed and the connectivity between all the monomers of the same polymer must be taken into account. Thus:

$$S(q,t)=\left\langle \sum_{p=p'} \sum\sum_{m\ m'} e^{iq\cdot[(R_p(0)+R_{pm}(0))-(R_{p'}(t)+R_{p'm'}(t))]} \right.$$

$$\left. + \sum_{p\neq p'} \sum_m e^{iq\cdot(R_p(0)+R_{pm}(0))} \sum_{m'} e^{-iq\cdot(R_{p'}(t)+R_{p'm'}(t))} \right\rangle \tag{15}$$

where m now sums over all N monomers in a polymer p. As $qR_g < 1$, with an experimental length scale larger than R_g, $q(R_p(t)+R_{pm}(t))$ can be approximated by $qR_p(t)$. $S(q, t)$ can now be approximated as:

$$S(q,t)\approx\left\langle N^2 \sum_{p=p'} e^{iq\cdot(R_p(0)-R_{p'}(t))} + N^2 \sum_{p\neq p'} e^{iq\cdot(R_p(0)-R_{p'}(t))} \right\rangle \tag{16}$$

In the reptation model where each polymer molecule is assumed to reptate through the other polymers, there is no correlation between the motions of the reptating molecule and those of the molecules which form the tube. Thus, while each molecule in the solution may be reptating, all other molecules which form its tube can be considered statistically fixed. It is reasonable, therefore, to assume that the centre of mass motions of different polymers are statistically independent. If this approximation is qualitatively correct:

$$S(q,t)\approx N^2N_pe^{-q^2D_s(1-\phi)t}+N^2\langle\rho'_p\rangle^2$$

$$=N^2N_pe^{-q^2D_s(1-\phi)t}+S_s(q) \tag{17}$$

Thus, by equations (14) and (17), D_c and D_s can be obtained by dynamic light scattering in the limits $t \ll t_R$ and $t \gg t_R$, respectively.

EXPERIMENTAL

*Materials**

The samples used in these experiments were prepared gravimetrically from sharp molecular weight fractions of polystyrene in spectroscopic grade cyclohexane which had been filtered through 0.5 μm Teflon filters (Millipore Co.). The aim was to investigate a wide range of molecular weights and concentrations; however, the solubility of polystyrene in cyclohexane placed significant limits on the experiments. Also, as the polymer is not expanded in the theta solvent, the semidilute region occurs at relatively high concentrations for a given molecular weight. Three samples of molecular weights 1.79×10^5 (NBS 705), 4.98×10^5 (Pressure Chemical), and 1.05×10^6 (NBS 1479) were used to study the concentration dependence. The total concentration range was from 37 to 280 mg cm^{-3} but for a given sample, the concentration was limited to a factor of 3 or 4. This range still provides almost two orders of magnitude change in D_s as shown by equation (10). Additional samples were prepared at 110 mg cm^{-3} from polymers with molecular weights 3.03×10^5 (hydrogenated polymer**), 3.9×10^5 (Pressure Chemical) and 9.67×10^5 (Waters Associates) to provide additional data on the molecular weight dependence of D_s. These polymers were in general not as well characterized or monodisperse as the first set. All preparations were sealed under vacuum in cylindrical sample cells with special care to avoid contamination by water. The samples were dissolved at 35°–40°C for two to six weeks with occasional gentle agitation. Only solutions which were optically clear, homogeneous and free of laser speckles were used in these experiments.

* Disclaimer: Certain commercial materials and equipment are identified in this paper in order to specify adequately the experimental procedure. In no case does such identification imply recommendation or endorsement by the National Bureau of Standards or does it imply that the material or equipment identified is necessarily the best available for this purpose.

** This sample is one of a polystyrene series prepared by Dr Y. Matsushita, Department of Synthetic Chemistry, Nagoya University, Japan

Methods

Dynamic light scattering measurements were carried out at 35.0°C using a goniometer and real time, multibit 128 channel autocorrelator (Malvern 7025) which have been described previously[13]. The scattering of vertically polarized 488 nm Ar ion laser light was measured at several angles within the range 30°–120° for each sample. At each angle the correlator sample time (also called lag time or delay time) was set for at least two widely different values. Typically, short times of 0.3–50 μs and long times of 1–100 ms were chosen such that the accumulated autocorrelation appeared as a single exponential with approximately 2 decay times measured. This corresponds to $\approx 85\%$ amplitude decay. Every experimental autocorrelation, when viewed without regard to the baseline reference calculated from the monitor channels, appeared as a single exponential. The short and long sample times generally differed by a factor of 10^2–10^6 and because of this wide separation the selection of sample times was usually as simple as it is for experiments on dilute, monodisperse samples.

Each autocorrelation decay was analysed by non-linear regression with a three parameter single exponential model function of the form:

$$C(q,t) = A + B\,e^{-\Gamma t} \qquad (18)$$

where $\Gamma = 2Dq^2(1-\phi)$. As it is known that the dynamic light scattering actually contains two distinct decays it is clear that treating the data in this manner involves two important approximations.

First, in fitting that data with the fast decay (short sample time), the baseline value A is allowed to float such that it is a sum of the infinite time baseline and the initial value of the slow decay. The assumption in this case is that the initial value of the slow decay is constant over several correlation times of the fast decay. For exponential functions separated in time by 10^2–10^6 this is a very good approximation. It is noteworthy that this assumption is often made, though perhaps unknowingly, in light scattering experiments where the 'infinite time' baseline is taken as the value of the correlator delay channels which are typically determined at delay times only twice the delay of the last point in the observed correlation function. For experiments such as these with two decays, the 'infinite time' baseline thus determined must include the true infinite time value plus an arbitrary contribution from the beginning of the slow decay. On the correlator used, the use of delay channels requires the loss of data channels. Thus the full 128 channels were chosen for the correlation function.

The second approximation is that in the measured correlation function of the slow decay any contribution from the fast decay process can be neglected. Again, because of the wide separation of sample times it is found that in the worst case the fast process contributes only 0.1% at the fourth point of the correlation function for the slow decay. By deleting the first 2 or 3 points from the analysis of the slow decays, extremely good single exponential fits to the data are obtained.

Each autocorrelation was accumulated for 30–150 min to provide sufficient counting statistics.

RESULTS

Figure 1 shows two representative autocorrelation functions which are obtained for a sample at two different

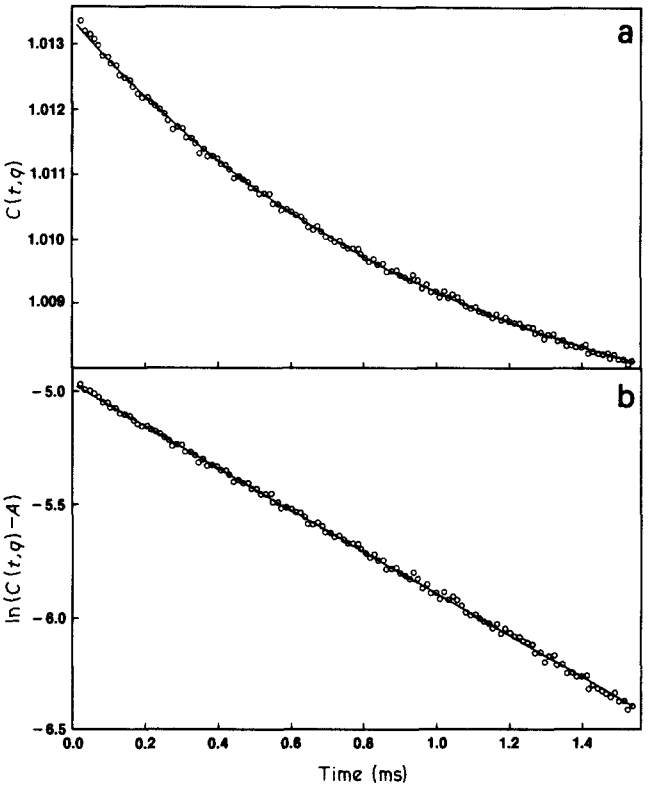

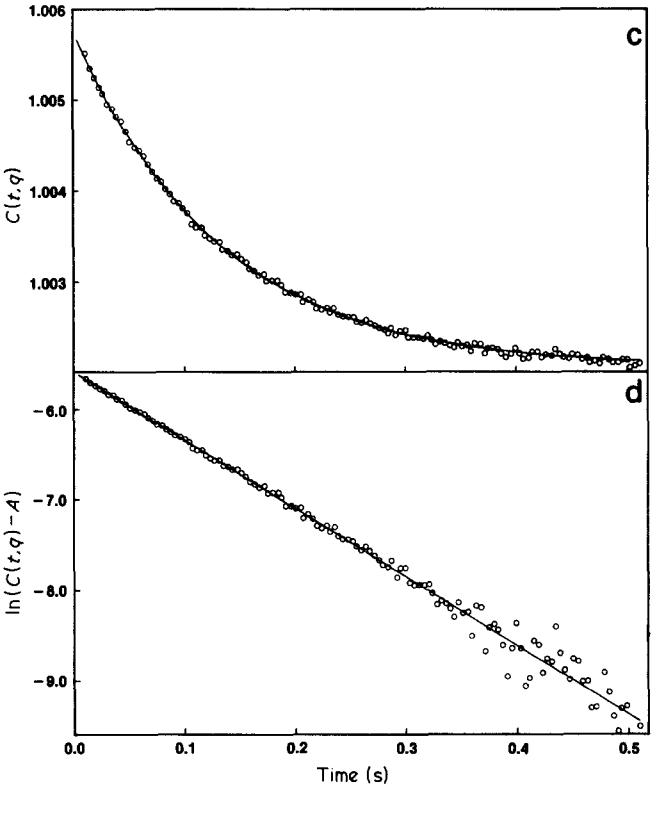

Figure 1 Correlation functions $C(q,t)$ from 1.05×10^6 molecular weight polystyrene in cyclohexane at a concentration of 45.5 mg cm^{-3} and with a scattering angle of 30° are shown in *Figures 1a* and *1c*. Solid curves represent the best fit using equation (18). The corresponding semilogarithmic plots are given in *Figures 1b* and *1d*. The two decay processes are seen separately by using experimental sample times of $\Delta t = 12\mu$s (*Figures 1a* and *1b*) and 4 ms (*Figures 1c* and *1d*)

correlator sample times. Each set is fitted to equation (18) as is shown by the solid curves in *Figures 1a* and *1c*. The adequacy of the single exponential approximation is shown by the quality of the fit and is demonstrated further in *Figures 1b* and *1d* where the same data is reduced and plotted as $\ln(C(t)-A)$ *versus* t. The deviations from single exponential behaviour are minor and the addition of an additional parameter in the form of a second-order cumulant fit (with floating baseline) produced essentially the same results and was not statistically justified.

The results of the short time correlation functions for a series of measurements varying from 30° to 120° are plotted in *Figure 2a* where the decay constants, Γ, are plotted against the appropriate scattering vector squared, q^2. D_c is obtained from the slope of this line. The analogous plot of the long time decays which yields D_s is given in *Figure 2b*. To within experimental error each plot shows rectilinear dependence of Γ on q^2 and has a zero intercept, both of which are indicative of a diffusion process. The resulting diffusion coefficients are plotted in *Figure 3* as log D_c and log D_s *versus* log concentration, for each of the three molecular weight samples.

The D_c results are examined first, as this is the quantity commonly studied by DLS. It is clear that the D_c results do not agree with the scaling predictions. From equation (4) the scaling prediction is that D_c should increase rectilinearly with concentration and should be independent of molecular weight. The results give not only a different power law (if there is a power law representation) but also molecular weight dependence. If the co-operative mode is interpreted by $D_c \propto N^x c^y$, the results of $0<x<0.7$ and $0<y<0.5$ are obtained instead of the scaling prediction of $D_c \propto N^0 c^1$. To emphasize the marked disagreement, dashed lines are drawn through each of the three molecular weight sets and a solid line of slope 1 for the scaling prediction. If the agreement with the scaling prediction was better for the highest molecular weight data if would have been possible to suggest finite molecular weight effects as an explanation for the disagreement. Instead, it seems that the trend is the opposite. An experimental power law dependence of D_c less than the prediction[3,4,6] is not unusual and has been reported for the majority of the DLS experiments in nominally good solvent systems. However, it is another matter for D_c to depend on the polymer molecular weight. By the scaling arguments D_c depends only on the mesh size, ξ_c (see equation (3)) and it is a basic tenet of scaling theory that in semidilute solutions (and certainly in highly entangled solutions such as these) the mesh size ξ_c must be independent of molecular weight. This is apparently the first report of D_c measurements by DLS in theta solutions. Agreement with scaling predictions for D_c in theta systems has been observed by sedimentation and gradient diffusion experiments[14,15]. One possible explanation for the discrepancy between DLS and these other, more macroscopic, techniques could be that in DLS the experimental distance and time scales are matched to the specific relaxation process which is being studied. In DLS the emphasis will be on localized regions and fluctuations of size ξ_c. It will procide, therefore, an extremely severe test of the step function approximations in the blob model. This is in contrast to the mesh sizes deduced from macroscopic quantities in experiments such as sedimentation and gradient diffusion. Perhaps a completely different average quantity could be involved. The step function approximation is considered in more detail later.

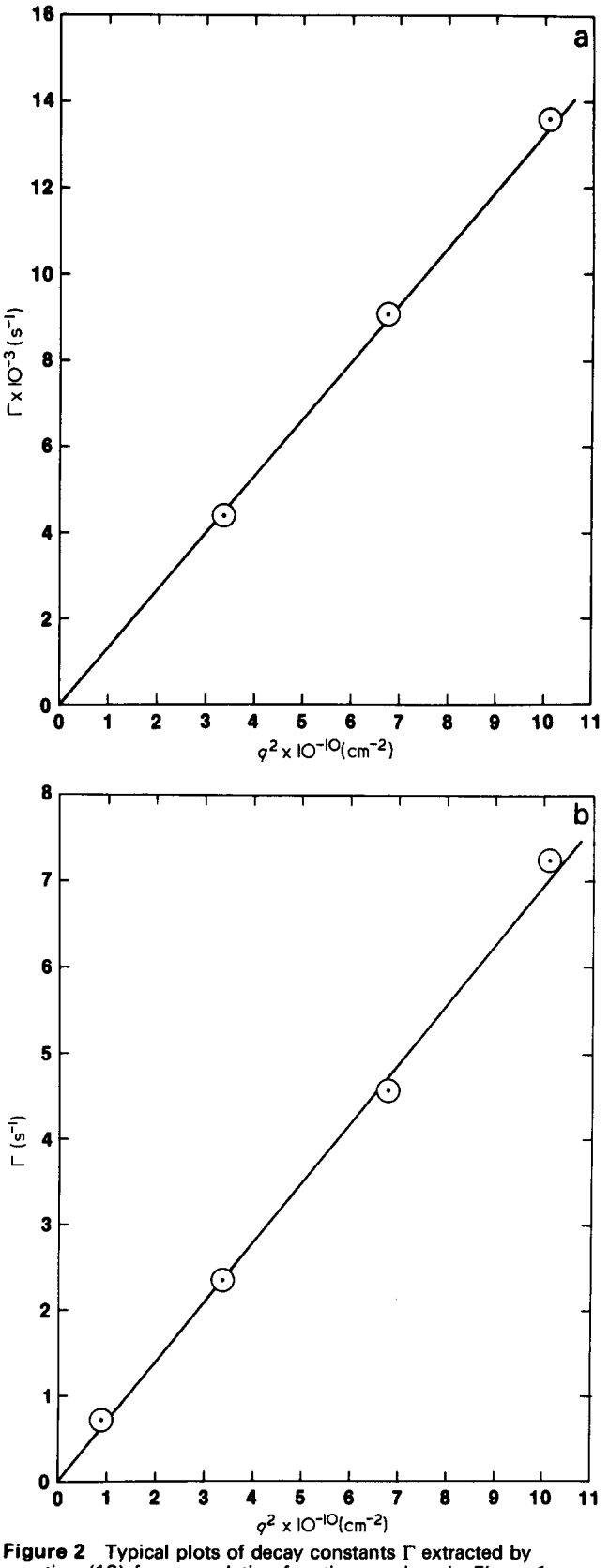

Figure 2 Typical plots of decay constants Γ extracted by equation (18) from correlation functions such as in *Figure 1 versus* scattering vector squared, q^2 are shown. Figures are for polystyrene of molecular weight 498×10^3 and include scattering angles from 30° to 120°. From the slope of the plot of the short decay constants, *Figure 2a*, D_c is determined while the long decay constants yield D_s. The factor $(1-\phi)$, where ϕ is the monomer volume fraction in solution, corrects the diffusion coefficients for backflow. (a) $D_c=\dfrac{\Gamma}{2q^2(1-\phi)}=1.5\times10^{-7}$ cm^2 s^{-1}; (b) $D_s=\dfrac{\Gamma}{2q^2(1-\phi)}=8.1\times10^{-11}$ cm^2 s^{-1}

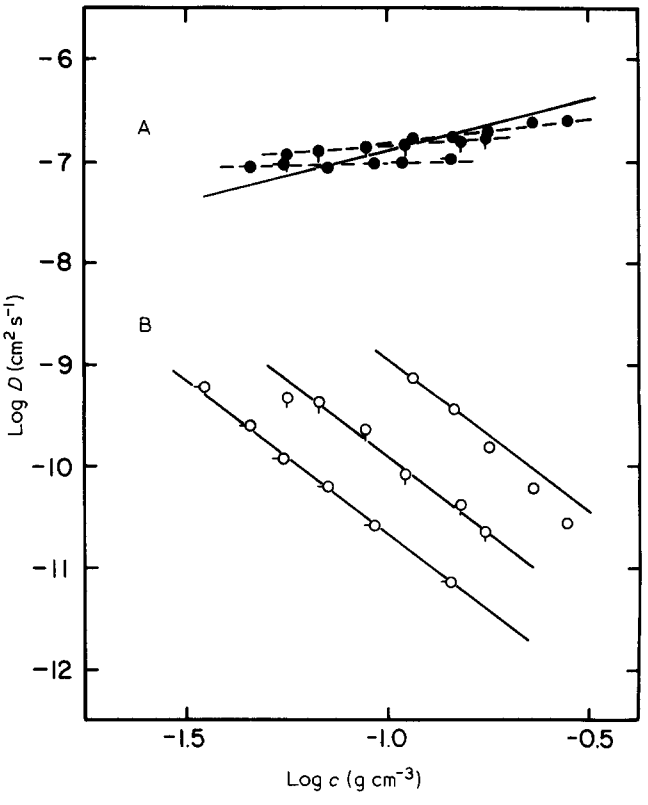

Figure 3 The changes of the co-operative diffusion coefficient (filled circles) D_c and the centre of mass diffusion coefficients (open circles) D_s are shown as a function of concentration for three molecular weight polystyrenes. Solid lines of slopes 1 (A) and −3 (B) show the scaling law predictions for D_c and D_s respectively. Three dashed lines indicate the actual concentration dependence of D_c for each of the molecular weights. $M \times 10^{-6}$; ○, 0.179; ○, 0.498; ○, 1.05

Nevertheless, there still is not an explanation for the molecular weight dependence of D_c.

However, the slow mode diffusion data are in very good agreement with the scaling law predictions of equation (10), as shown by the solid lines of slope −3 drawn through the data points. The dependence of D_s on polymer molecular weight is demonstrated in *Figure 4* where the average values of $\log D_s c^3$ are plotted for each molecular weight shown in the previous Figure along with three additional points taken at only one concentration (110 mg cm^{-3}), *versus* log molecular weight. The substantial agreement with the prediction from the reptation model is shown by a line of slope −2 drawn through the data. Having thus demonstrated the molecular weight dependence, *Figure 5* is a universal curve of $\log D_s M^2$ *versus* log concentration for all the theta solvent data, and the −3 line of the scaling prediction. For the concentration and molecular weight ranges studied here the dependence of D_s on c and M are well described by equation (10). As the scattering equations are based in part on assumptions of the scaling and reptation models, this agreement is basically a confirmation of the model's consistency, rather than a sufficient proof for the model.

Another expectation which is built into the model is that the theta solvent should provide a less ambiguous test of the scaling predictions than experiments in good solvents have provided. This is because the additional correlation length ξ_τ associated with the excluded volume may become greater than ξ_c, depending on temperature (solvent quality) and concentration. Previous work on the polystyrene–THF system was probably influenced by this effect. *Figure 6* is a plot of the polystyrene–THF data reduced as in *Figure 5*. It has been suggested[16] that despite the generally accepted good solvent quality this data shows crossovers from limiting good solvent behaviour ($D_s \propto c^{-1.75}$) to limiting theta behaviour ($D_s \propto c^{-3}$) as the polymer concentration increases. It is sufficient here to note that the theta solvent results, in contrast to the THF system, are in extremely good agreement with the model's predictions for all concentrations and molecular weights studied.

So far in this discussion the results have been considered only in relation to the predictions of scaling theory under the assumptions of the blob model. It is reasonable to propose this comparison as the derivation of the light scattering equations described previously is also based on the blob model approximation and reptation concept. Some shortcomings of the model are evident from the data. While it is significant that D_s measured at θ conditions gives quantitative agreement to the power law predictions, it is a problem that the D_c results disagree with the predictions. It is believed this is caused by some fundamental problems inherent in the blob–reptation model. First, while the step function approximation for the blob model may be good enough for calculating integrated quantities in the asymptotic limit, it is certainly not correct for the distances equal to or near ξ_c. This may be the reason that theoretical predictions are in better agreement with D_s than D_c measurements by DLS, and in even better agreement with sedimentation and gradient measurements. Second, the exact monomer

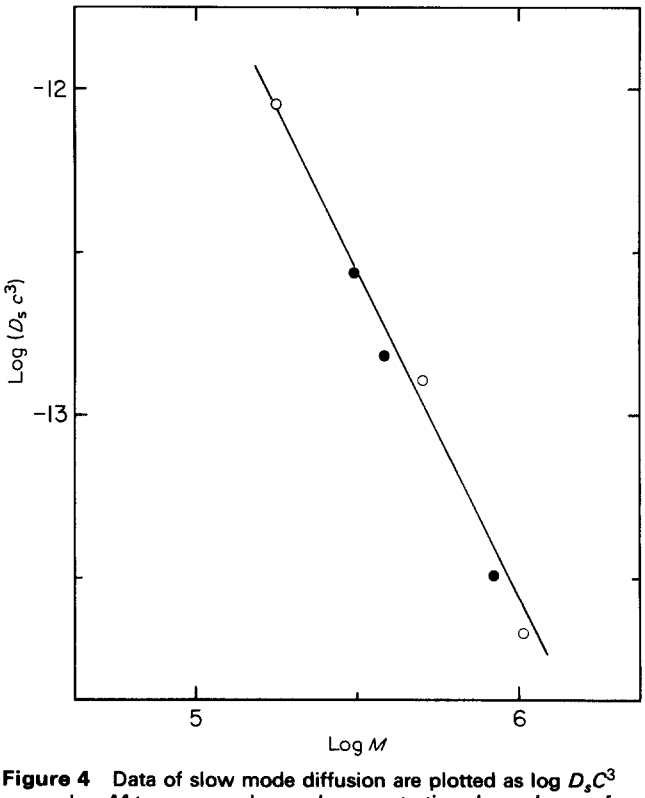

Figure 4 Data of slow mode diffusion are plotted as log $D_s C^3$ *versus* log M to remove observed concentration dependence of D_s and show molecular weight dependence only. Open circles are averaged values using all concentrations measured for the molecular weights shown in *Figure 3*. Filled circles are for three additional samples measured at approximately 0.11 g cm^{-3} only. The predicted power law slope of −2 for the reptation model for centre of mass diffusion is shown

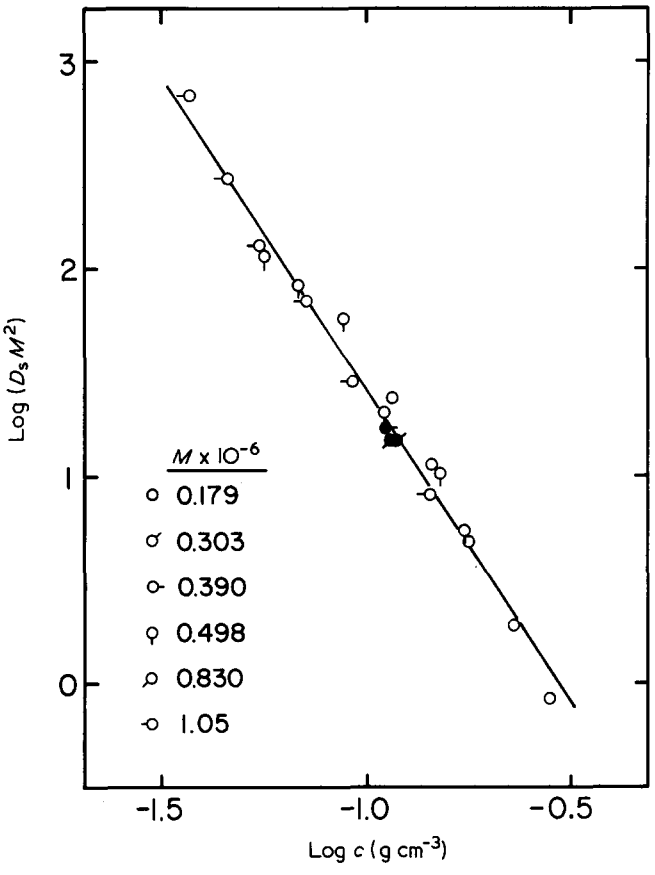

Figure 5 For six molecular weights D_s data from polystyrene in cyclohexane are reduced and plotted as log $D_s M^2$ *versus* log c. Filled circles as described for *Figure 4*. The scaling law slope prediction of -3 is shown

distribution (not only the cutoff) and hydrodynamic screening functions are not given. It is impossible to calculate the magnitude and the functional form of any measurable quantity. Thus, this model may have, for the first time, provided a simple physical representation and a qualitative explanation of a complex phenomena, but it does not provide quantitative predictions for an extended range in terms of concentration, temperature, or molecular weight. Until such predictions are possible, this problem cannot be considered solved.

In the meantime, comparison of these experimental results can be made with a more traditional approach which, while it may be more phenomenological, could be more quantitative. Thus, the formulation of Graessley[17,18] is used in which the monomeric friction coefficient (an average friction per monomer) remains as a phenomenological quantity. There is no attempt to relate this quantity to a blob size or hydrodynamic screening length. Therefore, the blob picture is not needed even though the reptation concept is retained. The concentration effects are considered in two ways. The first assumption is that in a semidilute solution of polymers which are not yet physically entangled (i.e. the concentration and molecular weight below those required for entanglement effects to be observed as a plateau modulus, for example) the centre of mass diffusion of a polymer chain can be modelled as a freely diffusing Rouse chain such that:

$$D^* = \frac{kT}{N\zeta_0} \tag{19}$$

where N is the degree of polymerization and ζ_0 is a concentration dependent (and molecular weight independent) monomeric friction coefficient.

As hydrodynamic interactions are assumed to be screened out in these solutions, this friction coefficient is equal to the friction that a single, unattached monomer would experience moving through the same solution. As the polymer molecular weight increases (holding the total mass concentration constant) its diffusion coefficient will decrease according to equation (19). However, when the molecular weight of the polymer attains some critical entanglement molecular weight, the topological constraints will confine the chain to diffuse by reptation. The friction on the chain is still $N\zeta_0$ (because the concentration has not changed) but the diffusion coefficient determined by that friction is now the coefficient for diffusion along the constrained tube:

$$D_t = D^* \tag{20}$$

These constraints are characterized by the primative path step length which, in the absence of the blob model, is identified as the end-to-end distance of the section of polymer chain between topological entanglements with molecular weight, M_e. M_e is traditionally defined experimentally from the onset of entanglement effects in viscoelastic measurements, such as a plateau zone in

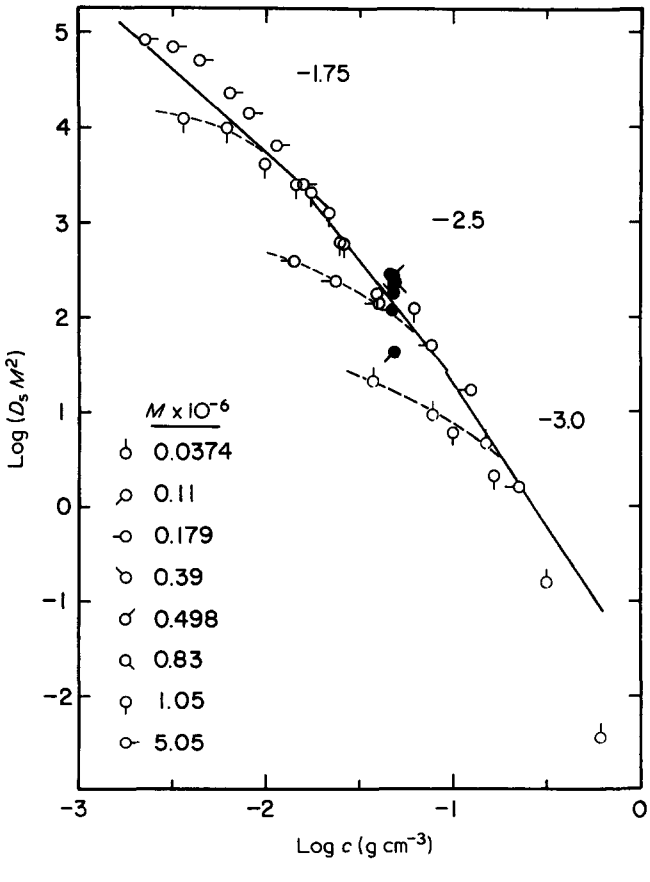

Figure 6 The D_s data for polystyrene in THF are reduced as in *Figure 5* and plotted *versus* log c. Lines showing the power law predictions for good solvent (-1.75), marginal solvent (-2.5) and theta solvent (-3) are indicated. Dashed curves through the lowest concentration points for three of the molecular weights indicate the failure of the model to produce a master curve.

modulus *versus* frequency. It is observed, at least for concentrated solutions, that M_e is inversely proportional to the volume fraction v of polymer such that:

$$M_e = M_e^0/v = M_e^0\rho/c \tag{21}$$

where M_e^0 is the entanglement molecular weight in bulk, ρ is the polymer density and c the mass concentration. Using the reptation model, the diffusion of a polymer in an entangled solution is then:

$$D_s = \frac{D_t}{3g} = \frac{kTM_0M_e}{3M^2\zeta_0} \tag{22}$$

where the average number of entangelements per polymer $g = M/M_e$ and M_0 is the monomer molecular weight. Combining equations (21) and (22) gives:

$$D_s = \frac{kTM_0\rho M_e^0}{3M^2c\zeta_0} \tag{23}$$

With this equation the magnitude and concentration dependence of ζ_0 can be calculated for all of the data, good solvent and theta solvent, using equation (19) for unentangled semidilute solutions and equation (23) for entangled solutions. It is expected[19] that ζ_0 will be proportional to the solvent viscosity η_s. *Figure 7* plots $\log \zeta_0/\eta_s$ *versus* $\log c$ for all the data from *Figures 5* and *6*. For the purpose of this plot, $M_e^0 = 18\,000$, $M_0 = 104$, $\rho = 1.05$ and the entanglement concentration $c_E = M_e^0\rho/M$.

Recent viscoelastic measurements by Osaki, Nishizawa and Kurata[20] provide an additional source of data for the concentration dependence of the monomeric friction coefficient. In their work shear relaxation moduli of concentrated polystyrene solutions were determined for large strains such that a material time constant τ_k was obtained which could be related to the equilibrium time of the contour length of the chain. Using Graessley's formulation[18] and the empirical results for τ_k the expression for ζ_0 is:

$$\zeta_0 = \frac{2\pi^2kT\tau_k}{3a_0^2P^2} \tag{24}$$

where P is the degree of polymerization $\left(=\frac{M}{M_0}\right)$ and a_0 is the effective monomer dimension (7.4×10^{-8} cm was used)[20]. Eight points are calculated from ref. 20 and included in *Figure 7* (filled circles); the viscosity of the Aroclor 1248 was 125 mN s m^{-2} [21].

This Figure, therefore, has the combined polystyrene data in three solvents, for molecular weights ranging from 37.4×10^3–8.42×10^6 g mol^{-1} and concentrations from 1.7×10^{-3}–0.63 g cm^{-3}. From this analysis the concentration dependence of the monomeric friction coefficient appears to be a smooth curve, independent of molecular weight, solvent quality, concentration regime and experimental technique. Even the absolute magnitude of ζ_0 is in reasonable agreement for all measurements at $c > c_E$. For $c < c_E$ the concentration dependence of ζ_0 follows the other three sets, but its magnitude seems to be too high. This is probably due to a breakdown in the approximation that polymer self diffusion can be modelled completely as free, Rouse-type diffusion for semidilute solutions with c below c_E. It is reasonable that even for concentrations below c_E entanglement effects could begin to interfere with the translational diffusion. Such a distinction between c_E for the onset of 'entanglement' effects in viscoelastic measurements and c^* for the onset of 'chain overlap' effects in hydrodynamic measurements has been proposed by Graessley[22] and also by Geissler and Hecht[23].

With this plot of the monomeric friction coefficient *versus* concentration, it would be useful to draw a curve through the data from an inclusive theory. Unfortunately, such a theory does not exist; the only option would be to combine various scaling laws with arbitrary magnitudes and crossovers, as in *Figure 6*. As the scaling laws rely on the blob model while the monomeric friction coefficient analysis does not, it would be inconsistent to apply those lines to this plot. Clearly, a more general theory is needed.

It is important to note that D_s (measured by DLS) is smaller by approximately a factor of 10 than the corresponding slowest diffusion coefficient measured by either pulse field gradient spin echo n.m.r.[24] or the new transient grating method, forced Rayleigh scattering, FRS[25]. At least in the case of FRS these measurements have been used to support the contention that in semidilute solutions mass transport occurs by reptation[25]. As the reptation model implicitly assumes that 1,2 correlations between polymer chains in semidilute solutions do not exist, it has been shown in this paper that DLS with $t > t_R$ should measure single chain centre of mass translational motion. Presently, there is no explanation of the observed factor of 10 difference between DLS results and n.m.r. and FRS results. If, as has been suggested[24], DLS is measuring an additional process which is slower than single chain mass transport (but nevertheless very closely related to self diffusion in terms of concentration and molecular weight dependences) the comparison *via* the monomeric friction coefficient suggests that viscoelastic experiments are also measuring this process.

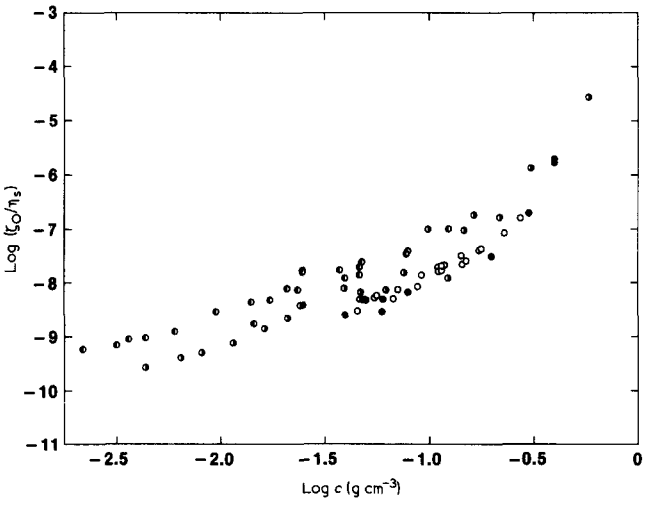

Figure 7 The monomeric friction coefficient ζ_0 is calculated according to Graessley[18] from D_s data above the entanglement concentration c_E (equation (23)) and below c_E (equation (19)) and from shear relaxation times τ_k above c_E (equation (24)). The concentration dependence of ζ_0 is observed in this plot of log ζ_0/η_s *versus* log c, where η_s is the solvent viscosity. All data for the concentrations and molecular weights in *Figures 5* and *6*, plus shear relaxation data from ref. 20 are included. Units are: ζ_0, 10^{-5} N s cm^{-1}; η_s, mN s m^{-2}; c, g cm^{-3}. ○, Cyclohexane, $c > c_E$; ◑, THF, $c > c_E$; ◐, THF, $c < c_E$; ●, Aroclor 1248, $c > c_E$

CONCLUSIONS

By dynamic light scattering it is possible to measure a centre of mass translational diffusion coefficient and the co-operative diffusion coefficient for semidilute polystyrene solutions. Under the assumptions of the blob model and reptation concept, the appropriate DLS equations can be derived to explain this observation. At theta condition the measured D_c depends on both concentration and molecular weight slightly, in an apparent contradiction to the scaling law predictions. However, the dependence of the slow mode diffusion coefficient on c and N are in complete agreement with scaling predictions of $c^{-3}N^{-2}$ for the self-diffusion coefficient.

Under an alternative interpretation the monomeric friction coefficient has been calculated from this D_s data in theta solvent and previous data in a good solvent, and also from viscoelastic experiments. Over the entire range of concentration and molecular weight the concentration dependence of all the sets of ζ_0 values is the same. The absolute magnitudes of ζ_0 from the different sets of data also agree to within a factor of 3.

ACKNOWLEDGEMENTS

The authors are indebted to Professor J. D. Ferry for suggesting the monomeric friction coefficient interpretation of the data and of the data from ref. 19. The authors also thank Professor W. W. Graessley for making available ref. 18 prior to publication.

Note added in proof: It now appears (Bachus, R. and Kimmich, R. *Polymer* 1983, **24**, 964) that a discrepancy in the magnitude of D_s, similar to that reported above, also exists between n.m.r. and i.r. microdensitometry for bulk polyethylene samples. The n.m.r. results are almost an order of magnitude faster than the self diffusion coefficients of Klein and Briscoe (*J. Proc. R. Soc. A* 1978, **365**, 53). Again the cause of the disagreement is unknown.

REFERENCES

1 Schaefer, D. W. and Han, C. C. in press
2 Adam, M. and Delsanti, M. *Macromolecules* 1977, **10**, 1229
3 Schaefer, D. W., Joanny, J. F. and Pincus, P. *Macromolecules* 1980, **13**, 1280
4 Yu, T. L., Reihanian, H. and Jamieson, A. M. *Macromolecules* 1980, **13**, 1590
5 Munch, J. P., Lemarichal, P. L. and Candau,S. J. *J. Phys. (Paris)* 1977, **38**, 1499
6 Munch, J. P., Candau, S., Herz, J. and Hild, G. J. *J. Phys. (Paris)* 1977, **38**, 971
7 Amis, E. J., Janmey, P. J., Ferry, J. D. and Yu, H. *Polym. Bull.* 1981, **6**, 13; Amis, E. J., Janmey, P. J., Ferry, J. D. and Yu, H. *Macromolecules* 1983, **16**, 441
8 de Gennes, P. G. 'Scaling Concepts in Polymer Physics', Cornell Univ. Press, Ithaca, 1970
9 Amis, E. J. and Han, C. C. *Polymer* 1982, **23**, 1403
10 de Gennes, P. G. *Macromolecules* 1976, **9**, 587; de Gennes, P. G. *Macromolecules* 1976, **9**, 594
11 Lodge, T. P., Han, C. C. and Akcasu, A. Z. *Macromolecules* in press
12 Daoud, M., Cotton, J. P., Farnoux, B., Jannink, G., Sarma, G., Benoit, H., Duplessix, R., Picot, C. and de Gennes, P. G. *Macromolecules* 1975, **8**, 804
13 Han, C. C. and Akcasu, A. Z. *Macromolecules* 1981, **14**, 1080
14 Nystrom, B. and Roots, J. *J. Macromol. Sci.-Rev. Macromol. Chem.* 1980, **C19**, 35; Vidakovic, P., Allain, C. and Rondelez, F. *Macromolecules* 1982, **15**, 1571
15 Roots, J. and Nystrom, B. *Macromolecules* 1980, **13**, 1595
16 Schaefer, D. W. personal communication
17 Graessley, W. W. *Adv. Polym. Sci.* 1974, **16**, 1
18 Graessley, W. W. *Adv. Polym. Sci.* 1982, **47**, 67
19 Ferry, J. D. 'Viscoelastic Properties of Polymers', 3rd Ed., John Wiley and Sons, New York, 1980
20 Osaki, K., Nishizawa, K. and Kurata, M. *Macromolecules* 1982, **15**, 1068
21 Osaki, K. personal communication
22 Graessley, W. W. *Polymer* 1980, **21**, 258
23 Greiesler, E. and Hecht, A. M.; 509, Proceedings, IUPAC Macro 82
24 Brown, W., Johnsen, R. M. and Stilbs, P. *Polymer Bulletin* 1983, **9**, 305
25 Leger, L., Hervet, H. and Rondelez, F. *Macromolecules* 1981, **14**, 1732